Source Characterization of Atmospheric Releases using Quasi-Random Sampling and Regularized Gradient Optimization

Bhagirath Addepalli, Christopher Sikorski, and Eric R. Pardyjak

UUCS-09-001

Department of Mechanical Engineering
School of Computing
Department of Mechanical Engineering
University of Utah
Salt Lake City, UT 84112 USA

January 28, 2009

Abstract

In the present work, an inversion technique to solve the atmospheric source characterization problem is described. The inverse problem comprises characterizing the source (x, y and z coordinates and the source strength) and the meteorological conditions (wind speed and wind direction) at the source, given certain receptor locations and the concentration values at these receptor locations. A simple Gaussian plume dispersion model for continuous point releases has been adopted as the forward model. The solution methodology for this nonlinear inverse problem consists of Qausi-Monte Carlo (QMC) sampling of the model parameter space and the subsequent application of gradient optimization. The purpose of conducting QMC sampling is to provide the gradient scheme a good initial iterate to converge to the final solution. A new misfit functional that computes the L_∞-norm of the ratio of the observed and predicted data has been developed and was used in the QMC search stage. It has been demonstrated that the misfit functional developed, guides the inversion algorithm to the global minimum. Quasi-random sampling was performed using the Hammersley point-set in its original, scrambled and randomized form. Its performance

was evaluated against the Mersenne-Twister uniform pseudo-random number generator in terms of the speed and quality of the initial iterate provided. Regularized Newton′s method with quadratic line-search was employed for gradient optimization. The standard Tikhonov stabilizing functional was used for regularization and the regularization parameter was updated adaptively during inversion. The proposed approach has been validated against both synthetic and field experiment data. Results obtained indicate that the proposed approach performs exceedingly well for inverse-source problems with the Gaussian dispersion equation as the forward operator. Also, the work presented highlights the advantages of using deterministic low-discrepancy sampling compared to the conventional pseudo-random sampling to solve the source-inversion problem.

Source Characterization of Atmospheric Releases using Quasi-Random Sampling and Regularized Gradient Optimization

Bhagirath Addepalli[1], Christopher Sikorski[2] and Eric R. Pardyjak[1]

Department of Mechanical Engineering[1], University of Utah

School of Computing[2], University of Utah

Abstract

In the present work, an inversion technique to solve the atmospheric source characterization problem is described. The inverse problem comprises characterizing the source (x, y and z coordinates and the source strength) and the meteorological conditions (wind speed and wind direction) at the source, given certain receptor locations and the concentration values at these receptor locations. A simple Gaussian plume dispersion model for continuous point releases has been adopted as the forward model. The solution methodology for this nonlinear inverse problem consists of Qausi-Monte Carlo (QMC) sampling of the model parameter space and the subsequent application of gradient optimization. The purpose of conducting QMC sampling is to provide the gradient scheme a good initial iterate to converge to the final solution. A new misfit functional that computes the L_∞-norm of the ratio of the observed and predicted data has been developed and was used in the QMC search stage. It has been demonstrated that the misfit functional developed, guides the inversion algorithm to the global minimum. Quasi-random sampling was performed using the Hammersley point-set in its original, scrambled and randomized form. Its performance was evaluated against the Mersenne-Twister uniform pseudo-random number generator in terms of the speed and quality of the initial iterate provided. Regularized Newton's method with quadratic line-search was employed for gradient optimization. The standard Tikhonov stabilizing functional was used for regularization and the regularization parameter was updated adaptively during inversion. The proposed approach has been validated against both synthetic and field experiment data. Results obtained indicate that the proposed approach performs exceedingly well for inverse-source problems with the Gaussian dispersion equation as the forward operator. Also, the work presented highlights the advantages of using deterministic low-discrepancy sampling compared to the conventional pseudo-random sampling to solve the source-inversion problem.

Key words: Source characterization, Gaussian plume model, Quasi-Monte Carlo (QMC), Regularization, Newton's method, Line-search, Tikhonov stabilizing functional, Adaptive regularization

1. Introduction

The solution of inverse problems involves the retrieval of information about a physical process or phenomenon from known or observed data [46]. Inverse problems arise in various fields and hence techniques to solve such problems have been an area of extensive study. One of the contemporary applications of inversion techniques includes the source characterization problem for atmospheric contaminant dispersion. Atmospheric source characterization problems, also referred to as event reconstruction, source-inversion or inverse-source problems, comprise characterizing the source of a chemical / biological / radiological (CBR) agent released into the atmosphere. Source characterization typically involves predicting the release location and rate of the CBR agent and the meteorological conditions at the release site, based on the time-averaged concentration and wind measurements obtained from a distributed sensor network in the region of interest.

Efficient and robust event reconstruction tools can play a crucial role in the event of accidental or deliberate release of CBR agents in or close to urban centers. Under such circumstances, quick and accurate reconstruction can help government agencies evacuate people from the affected regions. Also, using the information obtained from inversion, forward models can be run to estimate the extent of the plume spread and the consequent exposure. Event reconstruction tools can also be of use to environmental monitoring agencies as they can help evaluate the contribution of the stack releases from various industries close to urban areas to the air quality within urban areas. Therefore, from the perspective of public safety and

national security, a fast, robust and accurate atmospheric event reconstruction tool is pivotal for air-quality management and to effectively deal with emergency response scenarios.

It is generally well accepted that there does not exist a single best procedure to solve an inverse problem. For inverse problems having small domains and few decision variables, conducting an exhaustive grid search is the most robust inversion technique [45]. For larger problems, the performance of a solution technique depends upon the problem at hand, the nature of the forward model and the manner in which the inverse problem is formulated. Inverse problems are also difficult to solve owing to their inherent ill posedness, i.e. the existence, uniqueness, and stability of the computed solution. For real-life inverse problems, the question of existence is more mathematical than physical [46, 35]. This is also true for the present case, wherein; the sensor network recording a hit suggests the existence of a solution to the source characterization problem. However, to date, there is no formal proof for the existence of solutions to inverse problems with contaminated data, and seldom do we obtain noise-free data from measuring devices [35]. Therefore, for the accurate retrieval of the model parameters (m), the knowledge of the uncertainty in the observed data (d_{obs}) is absolutely essential. In short, one needs to know the uncertainties (δ) in the data to know what it means to fit the data [35].

The solution phase of inverse problems can be divided into two stages [35]: 1) the estimation stage, and 2) the appraisal stage. The estimation stage involves using an inversion algorithm to predict a set of model parameters (m_{pr}) based on the observed data (d_{obs}). The appraisal stage is comprised determining how well the data generated (d_{pr}) using the predicted model parameters (m_{pr}) fits the observed data (d_{obs}) [46]. Errors arising in inversion and the inherent ill posedness associated with inverse problems can be accounted for in one of these two stages. Errors arising in the inversion procedure can be attributed to one of the four possible sources: 1) the forward modeling error (δ_{FM}), 2) measurement error (δ_M), 3) non-uniqueness, and 4) nonlinear error propagation. For real life problems, the forward modeling error (δ_{FM}) is inevitable. This is because no forward model (A) can ever incorporate all the physics associated with the problem. During inversion, the forward modeling (δ_{FM}) and the measurement errors (δ_M) are accounted for in the estimation stage. Non-uniqueness arises primarily due to one of the following four factors: 1) mapping of the infinite dimensional model space (M) to a finite dimensional data space (D) by the forward operator (A) 2) lack of information – this is especially true when solving an under-determined system, 3) correlation between the model parameters (m), and 4) distortion of the misfit functional due to the previously mentioned errors resulting in multiple optimal regions. Non-uniqueness and nonlinear error propagation (that is intractable) can be accounted for during the appraisal stage. Due to these uncertainties in the solution procedure, one usually defines a 'data-fit' or 'model-acceptancy' criterion (β) based on the prior information available about the noise level (δ) [6, 24, 27, 37]. In summary, the goal of inversion is to find a set of model parameters (m_{pr}) that fit the observed data (d_{obs}) to some prescribed level. All the solution techniques developed work on the same underlying principle - to reduce the misfit between the predicted (d_{pr}) and observed data (d_{obs}) using a suitable algorithm.

Given that the subject of source characterization of atmospheric contaminant dispersion is in its infancy, researchers have examined the applicability and effectiveness of the various available inversion procedures to solve such problems. The solution methodologies used span the range of deterministic (Adjoint methods), stochastic (Simulated Annealing (SA), Genetic Algorithms (GA), Bayesian inference using Markov Chain Monte Carlo sampling (MCMC)) and 'common-sense' methods (collector footprint methods). The inverse-source problem has been solved over local (micro and meso-scales), regional and continental scales for different model parameters (m) using empirical, diagnostic and prognostic models for scalar transport as the forward operator (A). Table 1 summarizes the salient features of the inversion procedures adopted by various research groups to solve the inverse-source problem.

As stated earlier, all inversion techniques have their own merits and demerits and the approaches found in Table 1 are no exception. Adjoint methods, apart from requiring a good initial guess, also require the misfit functional to be continuous and differentiable. Hence, they are more likely to get trapped in local minima, as, inverse problems are often characterized by misfit functionals that have multiple critical points (maxima, minima and saddle points). Also, for problems that have complicated forward operators (A) in the form of partial differential equations (PDE), Adjoint methods can get computationally expensive as they require the forward model evaluation and the Frechet evaluation over the entire domain on every

iteration (when Newton's method is employed, evaluation of the inverse of the Hessian over the entire domain is required). Therefore, problems that have complicated misfit functional surfaces often require stochastic sampling methods in order to distinguish the local minima from the global minima. The computational efficiency of guided-search algorithms such as SA and GA also depends upon the nature of the forward model (A), as, every iteration of these algorithms also requires the forward model (A) to be evaluated. Adjoint methods, SA and GA also carry the added disadvantage that they only provide a single model that fits the data rather than giving a set of acceptable models. Though Bayesian inference techniques appear robust and give probabilistic answers, they rely heavily upon the manner in which prior information is included into the initial probability distribution [31]. The posterior distribution is then computed using MCMC sampling, which also requires the forward model (A) to be evaluated on every iteration, and hence can get computationally intractable in higher dimensions owing to the 'curse of dimensionality' [35].

In this paper, an approach that has the combined benefits of stochastic sampling and gradient descent methods is presented. Stochastic sampling is performed using Quasi-Monte Carlo (QMC) and Monte Carlo Quasi–Monte Carlo (MC-QMC) point sets. It should be noted that the QMC search is not a guided-search and this ensures that the misfit functional space has been adequately sampled, thereby eliminating the possibility of getting stuck in a sub-optimal region. The objective of conducting quasi-random search is to provide the gradient optimization scheme a good starting solution. In order to make the QMC search procedure computationally inexpensive, a relaxed 'data-fit' criterion (β_{QMC}) is imposed. Gradient optimization is performed with the starting solution provided by the QMC search stage until the global minimum is reached. The Gaussian plume dispersion model has been adopted as the forward model (A) because of its theoretical and computational simplicity and the proposed approach has been validated using both synthetic and field experiment data (The Copenhagen Tracer Experiments – TCTE) [16].

Apart from the hybrid approach proposed, the present paper also investigates some of the vital aspects of the atmospheric source characterization problem when using the Gaussian plume model as the forward operator (A). The first feature examined is the effect of the misfit functional formulation on the accuracy and complexity of inversion. Some of the popular formulations of data-discrepancy functionals are based on the Euclidian norm of the misfit, Euclidian norm of the relative misfit, the Kullback-Leibler information divergence functional, and the negative Poisson log-likelihood functional [42]. Misfit functionals based on the L_2-norm are often used when the errors (δ) included in inversion are assumed to be additive in nature. Misfit functionals based on the relative error are adopted when the uncertainties (δ) are incorporated as multiplicative errors [7]. Due to the costs involved with placing and monitoring the sensors in cities, atmospheric source inversion problems always suffer from a sparse number of measurements (N). The accuracy of most of the techniques found in Table 1 is directly related to the number of non-zero measurements recorded by sensors. Therefore, prior to solving the inverse problem, the role of the misfit functional formulation on the number of measurements (N) required in general and the number of non-zero measurements required in particular was investigated. Based on this study, it was concluded that the accuracy of inversion with data-discrepancy functionals based on the absolute and relative misfit depended strongly on the number of non-zero measurements available. Therefore, a new misfit functional that computes the L_∞-norm of the ratio of the observed data (d_{obs}) and predicted data (d_{pr}) and equally-weights sensors with zero-hits was developed. This functional was used in the QMC search stage with the relaxed 'data-fit' criterion (β_{QMC}) ($\beta_{QMC} = d_{obs} / d_{pr}$). It is suggested that in atmospheric event reconstruction problems, sensors with non-zero measurements help identify a set of optimal regions in the solution space, while sensors with zero-hits help locate the optimum region from the various sub-optimal regions. Since the misfit functional developed weighs all sensor measurements equally, the possibility of uniquely identifying the source parameters (m) using this formulation is higher when compared to the traditional formulations. As gradient optimization methods work only for a convex misfit functional, the conventional misfit functional based on L_2-norm of the difference between the observed (d_{obs}) and predicted data (d_{pr}) was used in the descent procedure.

The second feature examined was the performance of the various QMC point sets in the stochastic sampling procedure. QMC sampling was preferred over the conventional MC sampling as QMC point-sets have been specifically designed to improve upon the MC estimates through the suitable specification of a point-set [17]. Quasi-random numbers were developed to fill an s-dimensional hypercube $[0,1)^s$ more

uniformly than the traditional pseudo-random numbers. To ensure that the misfit functional space is adequately sampled, QMC point-sets were employed. Several point-sets (e.g. Halton, Hammersely, Sobol, ShiftNet and NiederreiterXing) were considered in their original, scrambled and randomized forms (MC-QMC) and their performance was evaluated in terms of the speed and quality of the initial guess (m_{QMC}) provided to the optimization scheme. Of all the point-sets, the Hammersley sequence was found to be the most efficient in terms of the number of search points required for providing a starting solution. Hence, for conciseness, only these results in comparison to the Mersenne-Twister generator are presented.

The choice of the descent methods, stabilizing functional and the regularization parameter (α) for gradient optimization were also examined. Newton's method is an attractive choice for the current problem as an analytical expression for the Frechet and the Hessian can be pre-computed for the Gaussian plume equation. Also, since the size of the Hessian matrix for the present problem is relatively small (=5×5), its inverse can be computed quickly and accurately. The regularized version of Newton's method with quadratic line-search was implemented with the standard Tikhonov stabilizing functional. The regularization parameter (α) was updated adaptively in these algorithms. Several other features that play a significant role in inversion in general and atmospheric source characterization problems in particular were investigated, but are not discussed to aid conciseness.

As has been the central theme of this discussion, the area of application of inversion techniques to atmospheric source characterization problems is in its nascency and various methods are being tested and their performance is being evaluated. In the work presented in this paper, a solution procedure that is different from the ones published in the literature is suggested. As with most of the other inversion techniques, the speed and accuracy of the present solution methodology depends on the noise-level (δ) in the observed data (d_{obs}) and the quality of the forward model (A). When properly formulated, the solution to an inverse problem can help identify the necessary physics that need to be incorporated into the forward model (A). Thus, inverse problems can in-turn be used to improve the speed and accuracy of the solution to the forward problem by enhancing or pruning the forward model (A).

2. Problem Definition

2.1. The Forward Problem

The Gaussian plume model (GPM) is the simplest model that describes the dispersion of atmospheric contaminants. It is an analytical expression which is a special solution to the advection-diffusion equation [8,25,41]. Of all the models used to characterize atmospheric dispersion, the GPM takes the least execution time. In emergency-response situations, the two most important factors are the speed and accuracy of reconstruction. The accuracy of reconstruction depends as much on the forward model (A) as it does on the inversion technique. Therefore, within its range of applicability, the GPM is the most desirable in such situations, due to the meager cost associated with the forward model evaluation. Accordingly, the inverse-source problem has been solved using the GPM for continuous point-releases as the forward operator (A). The GPM for steady, continuous and uniform wind conditions can be written as:

$$C_R(x_R, y_R, z_R) = \frac{Q_S}{2 \cdot \pi \cdot u_S \cdot \sigma_y \cdot \sigma_z} e^{-\frac{y^2}{2\sigma_y{}^2}} \cdot \left\{ e^{-\frac{(z_R - z_S)^2}{2 \cdot \sigma_z{}^2}} + e^{-\frac{(z_R + z_S)^2}{2 \cdot \sigma_z{}^2}} \right\} \tag{1}$$

$$\sigma_y = \frac{C_1 \cdot x}{\sqrt{1 + 0.0004 \cdot x}} \tag{1.1}$$

$$\sigma_z = C_2 \cdot x \tag{1.2}$$

$$x = -(y_R - y_S) \cdot Cos(\theta_S) - (x_R - x_S) \cdot Sin(\theta_S) \tag{1.3}$$

$$y = -(y_R - y_S) \cdot Sin(\theta_S) + (x_R - x_S) \cdot Cos(\theta_S) \tag{1.4}$$

Eqn. (1) gives an estimate of the concentration at a receptor (C_R) with the position vector $\vec{X} = \left[(x_R - x_S),(y_R - y_S),(z_R - z_S)\right]$; where, x_S, y_S, z_S, and x_R, y_R, z_R, represent the source and receptor coordinates respectively. The emission rate is Q_S and the wind speed (u_S) and direction (θ_S) are assumed to be constant over the region of interest. The distances ($x_R - x_S$), ($y_R - y_S$) and ($z_R - z_S$) are measured in the along-wind, cross-wind, and vertical directions with the origin of the coordinate system being the source location. σ_y and σ_z (Eqns. (1.1) and (1.2)) are called the Gaussian plume spread parameters and account for the turbulent diffusion of the plume. They are empirical parameters and are defined for various stability conditions. For the present problem, Brigg's formulae for Pasquill C-type stability conditions have been chosen. These parameters, however, are very problem dependent and therefore for the present work, the empirical constants C_1 and C_2, which in Brigg's formulae are 0.22 and 0.20, have been replaced by 0.12 and 0.10 for TCTE [16] as per the work of [34]. There are several other assumptions that are tacit in the Gaussian dispersion equation for which the reader may refer to [8,41].

The forward problem can be defined as estimating the concentrations at the desired receptor locations based on the given model (source) parameters (m) and can be written as:

$$A(m) = d \tag{2}$$

$$m = \left[x_S \quad y_S \quad z_S \quad Q_S / u_S \quad \theta_S\right]^T_{5\times 1} \tag{2.1}$$

$$d = \left[C_{R1} \quad C_{R2} \quad . \quad . \quad . \quad . \quad C_{RN}\right]^T_{N\times 1} \tag{2.2}$$

where, A is the forward modeling operator (which in this case is the GPM), m is the set of model or source parameters, and d is the vector of concentration measurements at the various receptor locations.

2.2. The Inverse Problem

The inverse problem can be defined as the solution of the operator equation:

$$d = A(m) \tag{3}$$

The solution to the inverse problem comprises of determining a model 'm_{pr}' (predicted model) that generates predicted data, 'd_{pr}', which 'fits-well' the observed data 'd_{obs}'. Since the forward operator (A) is nonlinear, the solution to the inverse problem can only be found iteratively. Therefore, nonlinear inverse problems are often cast as minimization or optimization problems as shown below:

$$\arg\left(\min_{m_{pr}} \left\| A(m_{pr}) - d_{obs} \right\|^2 \right) \tag{4}$$

Since the source strength (Q_S) and the wind velocity at the source (u_S) are a fraction of each other in the Gaussian equation, more often than not, they cannot be retrieved uniquely. Therefore, they have been combined into a single term (Q_S / u_S) in the inversion procedure.

3. Validation Tests - *The Copenhagen Tracer Experiments – (TCTE)*

Data from the Copenhagen field experiments [16] has been used for the experimental validation of the proposed approach. As part of this experiment, the tracer sulphurhexafluoride (SF_6) was released without buoyancy from a tower of height 115 m. It was collected 2 – 3 m above the ground-level by sensors placed in three crosswind arcs positioned 2 – 6 km from the point of release. A total of 137 tracer-samplers were used with 48 sensors placed in the arc closest to the source (Arc 1), 43 in the arc farthest from the source (Arc 3) and 46 in the intermediate region (Arc 2). Three consecutive 20 minute averaged tracer

concentrations were measured, allowing for a total sampling time of 1 hour. The site was mainly residential having a roughness length (z_0) of 0.6 m. The experiment was conducted on different days under neutral and unstable stability conditions. For the present work, the experiment conducted on October 19, 1978 / 1979 has been considered. The experiment was conducted mid-day thereby resulting in unstable conditions (Monin-Obukhov length L ~ -108 m, friction velocity $u_* \sim 0.39$ m / s, inversion height ~ 1120 m, standard deviation of the lateral and vertical velocities at the release point $\sigma_v \sim 0.85$ m / s and $\sigma_w \sim 0.68$ m / s, Stability class = Pasquill C–type) . The emission rate was 3.2 g / s and the limit of estimation (LOE) of the sensors was 9 ng / m^3. The average temperature (t_S), wind speed (u_S) and direction (θ_S) at the release height during the course of the experiment were $t_S \sim 283.72$ K, $u_S \sim 4.92$ m / s and $\theta_S \sim 308.57$ degrees. For the validation of the numerical experiments, the height of the sensors was considered to be 2.5 m.

It is worth noting that for the October 19 experiment, 34 out of the 137 sensors received a hit. These have been denoted by the 'squares' (□) in Fig. 1. As stated in the introductory section, the total error that needs to be accounted for during the estimation stage is the sum of the following individual error components:

Estimation error (δ_E) = Forward modeling error (δ_{FM}) + Measurement error (δ_M)

Since the authors of the report make no mention of the uncertainties in the measurements, δ_E has been considered to be a result of δ_{FM} (i.e., δ_M=0). In order to quantify δ_{FM} when using the GPM, the forward problem was solved with the known source parameters. The results obtained are shown in Fig. 1. From the figure it is evident that despite using the modified σ_y and σ_z, the plume spread predicted by the GPM does not match the experimental measurements. *Therefore, it should be noted that the results obtained after inversion will not match the true source parameters.*

The difference in the plume spread predicted by the GPM can be attributed to the complexities associated with real-world flows that have not been incorporated into the present version of the GPM. Since $\delta_E = \delta_{FM}$, and δ_{FM} is due to the inadequacies of the forward model (A), the inversion procedure has been designed to drive the forward model (A) to match the zero and non-zero measurements recorded by the sensors. That is, the inversion procedure adopted ensures that at the end of inversion, the plume spread predicted by the GPM is as close as possible to that observed in the experiments, not in magnitude, but, in terms of the zero and non-zero measurements recorded by the respective sensors. And as stated above, the final predicted model parameters (m_{pr}) will not match the true source parameters (m_t).

4. Solution Procedure

4.1. *The Tikhonov Parametric Functional*

In a general setting, the solution to an inverse problem can be obtained by minimizing the following unconstrained parametric functional [46]:

$$P^{\alpha}(m_{\alpha}, d_{\delta}) = \mu_D^2(A(m_{\alpha}), d_{\delta}) + \alpha \cdot s(m_{\alpha})$$
$$\arg\left(\min_{m_{\alpha}} \left(P^{\alpha}(m_{\alpha}, d_{\delta}) \right) \right) \tag{5}$$

This can also be written as:

$$p(\alpha) = i(\alpha) + \alpha \cdot s(\alpha) \tag{6}$$

where $i(\alpha) = \mu_D^2(A(m_{\alpha}), d_{\delta})$ is the misfit functional, $s(\alpha) = s(m_{\alpha})$ is the stabilizing functional, and $p(\alpha) = P^{\alpha}(m_{\alpha}, d_{\delta})$ is the parametric functional. The parametric functional $p(\alpha)$ is a linear

combination of the misfit and the stabilizing functionals, and the unknown real parameter α is called the regularization parameter.

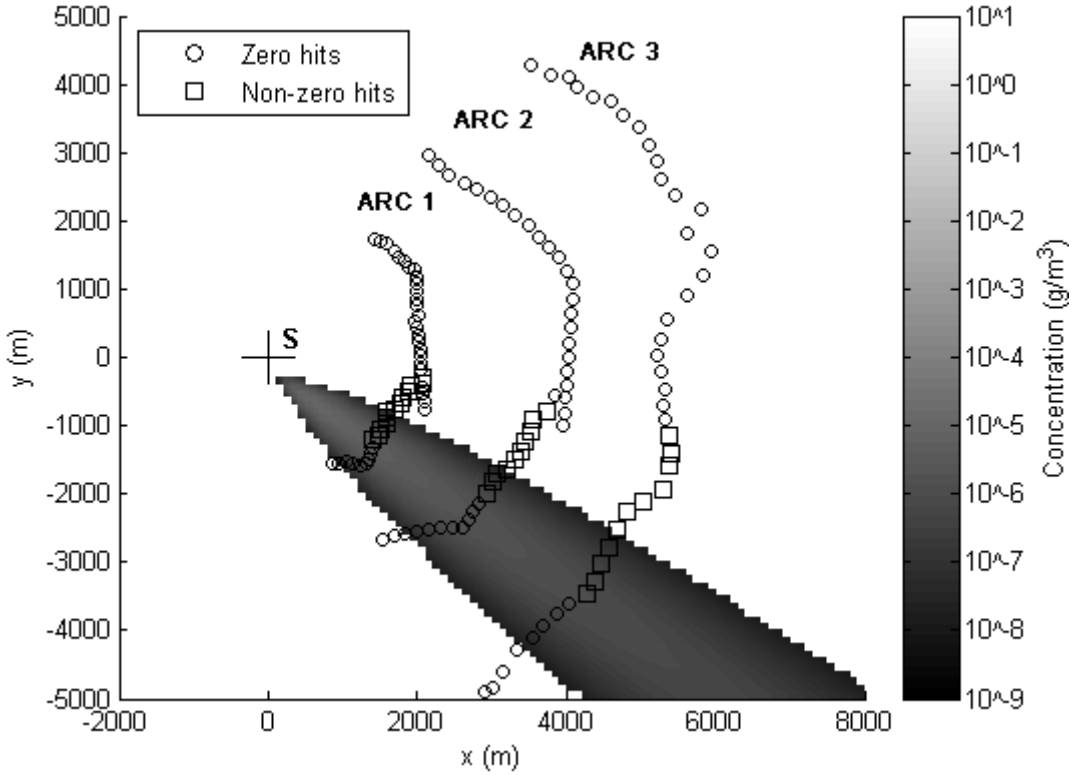

Fig. 1: Schematic depicting the sensor positioning and the number of zero (o) and non-zero (□) measurements recorded for TCTE on October 19. Also shown is the plume spread predicted by the GPM for true source parameters (m_t). 'S' is the true source location

The parametric functional described in Eqn. (5) can be minimized using different techniques. Depending upon the technique chosen, the inversion procedure acquires its respective name (such as GA, SA, MCMC sampling, gradient descent, adjoint methods, etc.). The role of the misfit functional $i(\alpha)$ is to check if, on every step of inversion, the discrepancy between the observed and the predicted data ($\left\| d_{obs} - d_{pr} \right\|; d_{pr} = A(m_{pr})$) is increasing or decreasing. Since most real-life inverse problems are ill-posed, casting the inverse problem as the minimization of the misfit functional can result in unstable solutions. This is because the operator A^{-1} may not be continuous over the entire model space M. The inherent ill-posedness of inverse problems can be overcome by considering a family of well-posed problems $(d = A_\alpha(m))$ that approximate the original ill-posed problem $(d = A(m))$. The scalar parameter $\alpha > 0$ in the above expression is called the regularization parameter and regularization is imposed under the constraint $m_\alpha \to m_t; as \alpha \to 0$ (where m_t is the true solution). That is, regularization approximates the non-continuous operator A^{-1} by the family of continuous operators $A_\alpha^{-1}(d)$ for different values of α. The family of continuous $A_\alpha^{-1}(d)$ operators that approximate the original non-continuous operator A^{-1} are called the regularization operators R_α $(R(d,\alpha) = A_\alpha^{-1}(d))$. Regularization operators can be constructed by adding a stabilizing functional $s(\alpha)$ to the misfit functional $i(\alpha)$. The task of the stabilizing functional is to help identify from the set of all possible models

that fit the data, a solution, that belongs to the correctness-set M_C $(M_C \subset M)$, such that, the operator A^{-1} is continuous over M_C. Formulating an inverse problem in this manner converts an ill-posed problem into a 'conditionally-well-posed problem' expressed by the parametric functional in Eqn. (5).

In this paper, Eqn. (5) has been minimized using gradient descent methods. Gradient methods require the misfit functional to be convex, continuous and differentiable (C-C-D) to converge to the global minimum. Examining the GPM, one can recognize that the misfit functional generated by the GPM (using Eqn. (10)) has multiple critical points (maxima, minima and saddle points). In fact, when using the GPM, the number of global maxima (= ∞) in the misfit functional space is equal to the number of sensors (N) in the domain. This can be shown by considering the GPM in Eqn. (1). It can be seen that $x_S = x_R \; and \; y_S = y_R \Rightarrow C_R(x_R, y_R, z_R) = \infty$. The presence of 'N' global maxima in addition to the various error components (δ_E and δ_A) results in the formation of several critical points interspersed around the global minimum. Therefore, to employ gradient schemes to solve such problems, a good starting solution is pivotal. This starting solution needs to be in the C-C-D region surrounding the global minimum in the misfit functional space. If a starting solution in the C-C-D region can be identified, gradient descent methods are the most appealing of the available techniques, as, the analytical expressions for the Fretchet and the Hessian of the GPM can be pre-computed and used in the descent procedure. For this precise reason, the approach proposed in this paper comprises of QMC sampling to provide a good initial iterate to the gradient descent scheme.

In order to illustrate that the proposed approach works for inverse-source problems with the GPM as the forward operator (A), the domain of TCTE (Fig. (1)) was discretized and the misfit functional at every grid node was computed using Eqn. (10). This was done in 2D by considering the x and y coordinates of the source (x_S and y_S) to be the unknown model parameters (m). The results obtained are shown in Figs. 2(a) and 2(b). From the figures it can be seen that as $x_S \to x_R \; and \; y_S \to y_R, \left\| d_{pr} - d_{obs} \right\| \uparrow (increases)$. This behavior is in agreement with the above mentioned assertion that as $x_S \to x_R \; and \; y_S \to y_R, C_R(x_R, y_R, z_R) = d_{pr} \to \infty$. From the figures it can also be deduced that there exists a region in the misfit functional space (translucent dotted circle and triangle in Figs. 2(a) and 2(b)), which is convex and continuous, and houses the global minimum. The plots also shed light on the distortion of the misfit functional by the forward modeling error 'δ_{FM}' (assuming δ_M = 0). The distortion manifests in terms of the discrepancy observed in the predicted 'S_p' (square - □) and the true source locations 'S_t' (diamond - ◊) as shown in Fig. 2(b). However, not too many conclusions should be drawn from these plots as these are in 2D. In 5D, the hyper-volume that spans the C-C-D region might be of different size and corrugated, due to the effects of nonlinear error propagation.

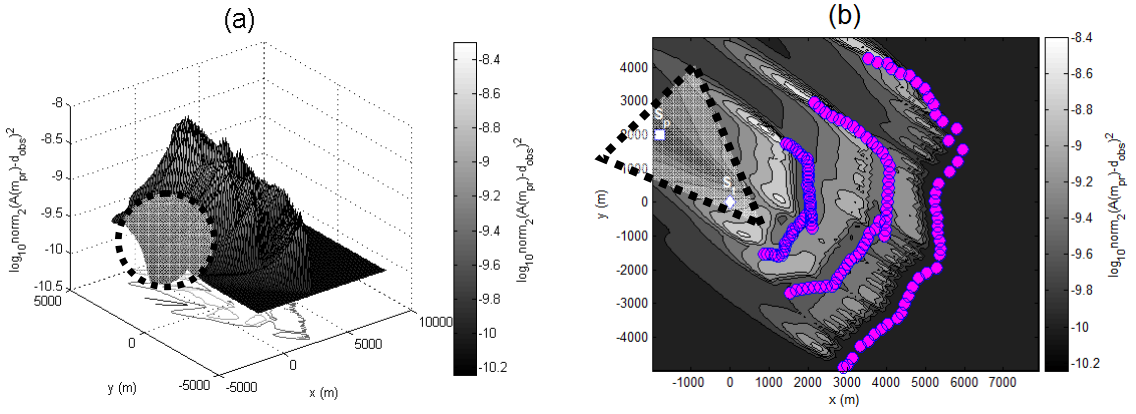

Fig. 2: (a) Surface of the misfit functional for TCTE, (b) 2D contour of the misfit functional for TCTE with the true (S_t) and predicted (S_p) source locations

4.2. *QMC and MC-QMC Sampling*

QMC sampling was performed over the misfit functional space to identify a good starting solution for the descent algorithm. QMC sampling is recommended over conventional MC sampling as quasi-random numbers were developed to fill an s-dimensional hypercube on $[0,1)^s$ more uniformly than pseudo-random numbers [14]. Additionally, QMC point-sets provide the extra advantage of being completely deterministic. This property of QMC point-sets is highly desirable for atmospheric event reconstruction problems. This is because, for known receptor locations, stochastic algorithms developed to solve the inverse-source problem for a real city can be tested for all possible model parameters and the performance of the algorithm in terms of total execution time (which is equivalent to the number of forward model evaluations) can be determined apriori. For the work presented in this paper, the Hammersley point-set in its original, scrambled and randomized form was considered. The performance of the point-set was evaluated with respect to the Mersenne-Twister generator, which is the standard uniform pseudo-random number generator used in most programming languages.

The Hammersley point-set is one of the most commonly used low-discrepancy point-sets in computer graphics. It is based on the radical inverse function in base b written as $\Phi_b(i)$. To compute the function value, the number i is written in base b and is then reflected about the radix point. For any base b, $\Phi_b(0) = 0$ and $\Phi_b(i) \in [0,1)$. Using the definition of $\Phi_b(i)$, for the d-th prime number p_d, the Hammersley point-set is written as [14]:

$$x_{i,d} = \begin{cases} i/N & d = 0 \\ \Phi(i)_{p_{d-1}} & otherwise \end{cases} \tag{7}$$

The scrambled version of the Hammersley point-set was obtained by applying Faure permutations over the original set [14]. The randomized form, also called MC-QMC, was computed using the Cranley-Patterson rotation [14]. The Cranley-Patterson rotation involves generating a random multidimensional vector $\vec{o}$ in the unit-hypercube $[0,1)^s$ and adding the vector to each of the components of the original Hammersley vector sequence ($\vec{x}$). The components of the newly generated sequence ($\vec{y}$) in the d-th dimension d are [14]:

$$y_{i,d} = (x_{i,d} + o_d) \bmod 1 \tag{8}$$

4.3. *The Misfit Functional*

The misfit functional is one of the most important components of an inversion algorithm. When properly formulated, it helps guide the inversion algorithm to the global minimum. Misfit functional formulation, just like the choice of an inversion algorithm, is highly problem-dependent. Most of the data-discrepancy functional formulations appearing in the atmospheric source-inversion problem literature [2,3,18,28,39,44] are either based on the L_2–norm (Eqn. (10)) or the log-likelihood of the misfit [34]. Misfit functionals based on the L_1-norm (Eqn. (9)) of the error have also been used in other areas of application of inversion techniques.

$$\rho_{L1}(A(m_{pr}), d_{obs}) = \left\| A(m_{pr}) - d_{obs} \right\|_1 \tag{9}$$

$$\rho_{L2}(A(m_{pr}), d_{obs}) = \left\| A(m_{pr}) - d_{obs} \right\|_2 \tag{10}$$

Computing the L_2–norm or the L_1–norm of the misfit to determine the class of models (m_{pr}) that fit the observed data (d_{obs}) can lead to erroneous results for the atmospheric source-inversion problem. This is

primarily because atmospheric inverse–source problems always suffer from sparse number of measurements (N) in general, and, very few non-zero measurements in particular. Therefore, computation of the L_1 or L_2 norms (Eqns. (9) and (10)) does not take into account the zero-hits recorded by the sensors, as, the magnitude of these norms are driven only by the non–zero measurements. Additionally, since these norms calculate the sum or sum of the squares of the misfits, they can give a misleading final misfit that satisfies the convergence requirements, but, might not correspond to a solution that is close to the true model (m_t). This has been demonstrated with the help of a simple 3D example with three receptors R1, R2 and R3 as shown in the Fig. 3(a). The unknown model parameters are assumed to be x_S, y_S and θ_S. Synthetic data was generated at these receptors with known source parameters. The inverse problem comprises of estimating the unknown model parameters from the computed concentration measurements at the receptors. Fig. 3(b) shows the plume spread predicted for the true source parameters (m_t) along the slice $\theta = 270°$. The true model parameters (m_t), observed data (d_{obs}) and the unknown model parameters (m) for this problem are:

$$m_t = \begin{bmatrix} 50 & 50 & 270^\circ \end{bmatrix}^T \qquad m = \begin{bmatrix} x_S & y_S & \theta_S \end{bmatrix}^T \qquad d_{obs} = \begin{bmatrix} 6.67 & 0 & 0 \end{bmatrix}^T$$

Since the domain is relatively small, the best procedure for inversion is performing an exhaustive grid search [45]. Conducting an exhaustive grid search and checking for zero-misfits will give multiple source locations that do not correspond to the true location (S). The first such scenario is shown in Fig. 3(c), wherein, if the misfit functional is formulated using Eqn. (9), multiple source locations along the sectors AR1B, CR2D and ER3F will give zero-misfits for various θ_S values. In fact, depending on the plume spread parameters C_1 and C_2, zero-misfits can be obtained along a sector of radius 'r' around the receptors R1, R2 and R3. Hence, it can be seen that for the simple 3D example, there exist several model parameters that satisfy the zero-error criterion. In the second scenario, having the source close to the origin with $\theta_S = 225°$ (i.e. the along the plane $\theta = 225°$) and using Eqn. (9) for the misfit will also result in a zero–misfit location close to the origin as shown in Fig. 3(d). Thus, based on this example it has been demonstrated that using Eqns. (9) and (10) for atmospheric event reconstruction problems might result in incorrect solutions.

To overcome this problem, a new misfit functional that takes into account both zero and non–zero hits and treats both of them equally is proposed in this paper. The new functional is based on the L_∞-norm of the ratio of the observed (d_{obs}) and predicted data (d_{pr}) and is shown in Eqn. (11.4) below. The constant ε ($\varepsilon << LOE$) accounts for the zero hits and becomes insignificant for non–zero hits.

$$d_{obs} = \begin{bmatrix} C_{R1} & C_{R2} & \cdot & \cdot & \cdot & \cdot & C_{RN} \end{bmatrix}^T_{N\times 1} \tag{11.1}$$

$$d_{pr} = \begin{bmatrix} \left(A(m_{pr})\right)_{R1} & \left(A(m_{pr})\right)_{R2} & \cdot & \cdot & \cdot & \cdot & \left(A(m_{pr})\right)_{RN} \end{bmatrix}^T_{N\times 1} \tag{11.2}$$

$$D_\varepsilon = \left[\frac{d_{obs_{R1}}}{d_{pr_{R1}} + \varepsilon} \quad \frac{d_{obs_{R2}}}{d_{pr_{R2}} + \varepsilon} \quad \cdot \quad \cdot \quad \cdot \quad \frac{d_{obs_{RN}}}{d_{pr_{RN}} + \varepsilon} \right]^T_{N\times 1} \tag{11.3}$$

$$\rho(A(m_{pr}), d_{obs}, \varepsilon) = \left\| D_\varepsilon \right\|_\infty \tag{11.4}$$

The applicability of the proposed misfit functional is based on the fact that for inversion without noise, the result of inversion should give the true model parameters (m_t), such that, in some sense, for $m_{pr} = m_t$, $d_{obs} / d_{pr} = 1$. Running the inversion algorithm until $\rho(A(m_{pr}), d_{obs}) \le \beta$ (where β is some constant) ensures that 'm_{pr}' is in the vicinity of 'm_t'. The scalar β is a problem-specific constant and its value depends upon the noise-level (δ_M) in the observed data (d_{obs}) and the number of available measurements (N). Therefore, for consistent or over-determined problems, β can be estimated as:

$$\beta = 1 + \delta_M + \kappa \tag{12}$$

where, δ_M is the measurement error and κ is a relaxation factor that takes into account the forward modeling error (δ_{FM}).

The new misfit functional was used in the QMC search stage to identify a good starting solution for the gradient descent scheme. The value of β characterizes the size of the hyper-volume constituting the C-C-D region around the global minimum in the misfit functional space. Setting $\beta = 1 + \delta_M$ would imply solving the inverse problem by pure quasi-random search, which can be very expensive. Therefore, based on a number of numerical experiments, a β value, referred to as β_{QMC}, was chosen for the QMC search stage that made QMC sampling extremely economical. Since gradient methods only work for convex misfit functionals, the conventional misfit functional based on L_2–norm (Eqn. (10) was used for computing the new iterates for the gradient scheme. However, the new iterates were accepted only as long as the value of β_{QMC} at each of the receptors was preserved or improved (β_{GD}).

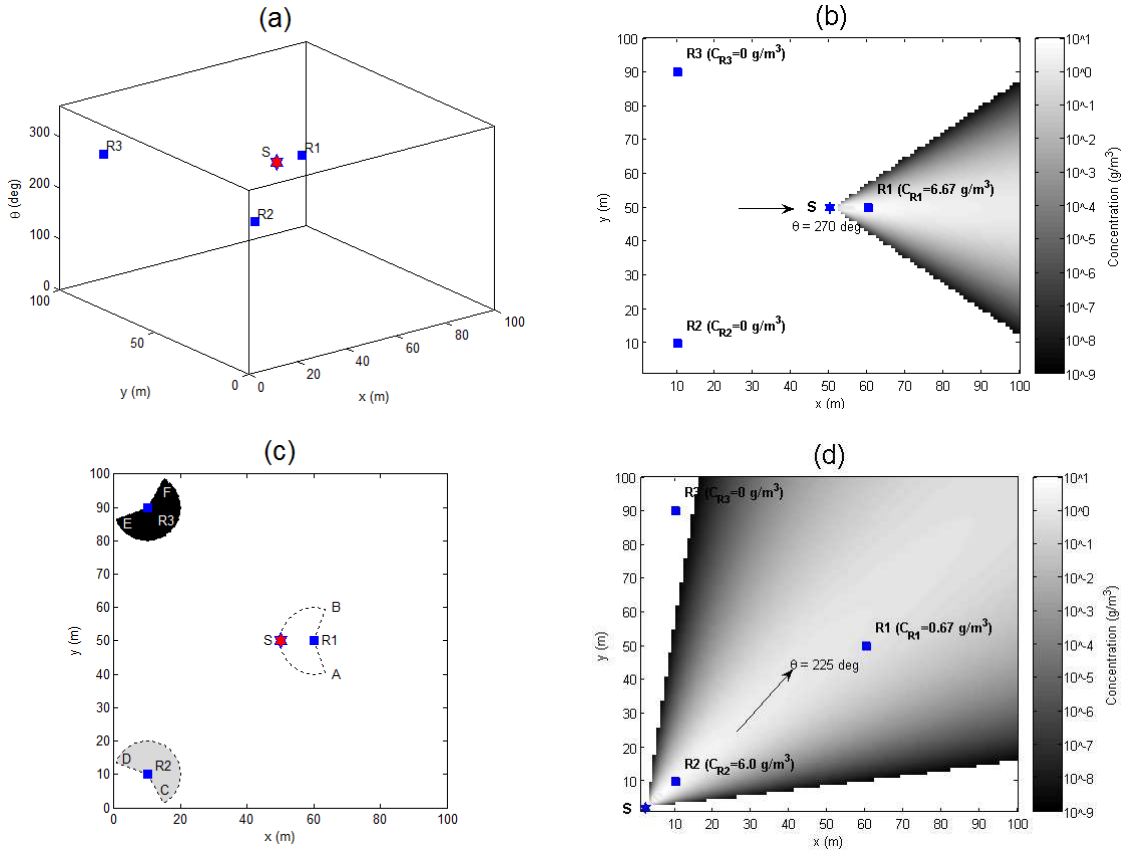

Fig. 3: (a) Source – Receptor configuration for the synthetic three parameter example problem, (b) Plume spread predicted by the GPM for true model parameters along θ = 270° plane, (c) Possible source locations (sectors AR1B, CR2D, ER3F) that yield zero-misfit based on the L_1-norm for various θ values , (d) Incorrect source location that yields zero-misfit based on the L_1-norm along the plane θ = 225°

4.4. *The Stabilizing Functional, Regularization Parameter and Newton's Method*

The stabilizing functional s(m) in conjunction with the regularization parameter α is used to construct the regularization operator R_α that converts an ill-posed problem into a 'conditionally-well-posed' problem. For the inverse-source problem, the standard Tikhonov stabilizing functional has been

chosen as the penalty functional. The Tikhonov stabilizer is shown in Eqn. (13) below. m_{apr} represents some prior information that we might have about the model parameters (m). No prior information was assumed in the solution procedure for the atmospheric event reconstruction problem. However, a modified version of the stabilizer shown in Eqn. (13) was used in the descent algorithm and is shown in Eqn. (14). The rationale behind using this stabilizer is based on the initial iterate provided by the QMC search stage. The QMC search stage was designed to provide a starting solution that belongs to the C-C-D hyper-volume around the global minimum. Therefore, to ensure that the gradient scheme does not bounce out of the C-C-D region, the model parameters on the current and previous iterations were used to stabilize the gradient scheme.

$$s(m) = \left\| m - m_{apr} \right\|_2^2 \tag{13}$$

$$s(m) = \left\| m_i - m_{i-1} \right\|_2^2; i = 2,3..... \tag{14}$$

The regularization parameter α determines the relative significance of the misfit and the stabilizing functionals. Choosing extremely small values of α leads to the situation where the inverse problem reduces to the minimization of the misfit functional, which can result in unstable solutions. Large values of α corresponds to the situation wherein the inverse problem is driven in the direction of the stabilizer. Hence, accurate reconstruction requires optimal regularization parameter selection. Several methods have been proposed for optimal regularization parameter selection. Prominent among these are the Mozorov condition [42] and the L-curve criterion [5, 40 42, 46]. In the present paper, a more heuristic approach as suggested in [46] has been adopted. The regularization parameter has been estimated following Eqns. (15) and (16) shown below. The first iteration of the gradient scheme is run without regularization and α_1 is calculated at the end of the iteration following Eqn. (15). Values of α on the subsequent iterations are computed using Eqn. (16). The value of the scalar q helps control the extent of regularization. Lower values of q favor faster convergence, but, can lead to instabilities in the inversion procedure. Higher values of q promote better stability, but result in more iterations for convergence.

$$\alpha_1 = \frac{\left\| A(m_1) - d_{obs} \right\|_2^2}{\left\| m_1 - m_0 \right\|_2^2} \tag{15}$$

$$\alpha_i = \alpha_1 \cdot q_{i-1}; \ (0 < q < 1); \ i = 2,3,..... \tag{16}$$

Following Eqns. (10), (14), (15) and (16), the unconstrained parametric functional described in Eqn. (5) can be written as:

$$P_i^{\alpha}(m_{\alpha}, d_{\delta}) = \left\| A(m_i) - d_{obs} \right\|_2^2 + \alpha_i \cdot \left\| m_i - m_{i-1} \right\|_2^2 \tag{17}$$

The parametric functional shown in Eqn. (17) has been minimized using Newton's method. To ensure convergence and to prevent overshooting of the Newton jump, quadratic line-search was implemented. For computational efficiency, the Hessian was approximated by calculating the residual assuming unit-step with linear line-search. The details of the algorithm implemented can be found in [46].

5. Results and Discussion

As stated in the previous sections, the algorithm developed to solve the inverse-source problem comprises of quasi-random sampling of the model parameter space and the subsequent application of regularized Newton's method with quadratic line-search. Quasi-random sampling was performed to provide a good starting solution for the gradient scheme and the Hammersley point-set in its original,

scrambled and randomized form was used for this purpose. The results obtained by implementing the algorithm are displayed in Table. 2. To improve the stability of the gradient scheme, the x and y-axes of the 5D coordinate system were translated from (0,0) to (2000,5000) during inversion. 'm_t' represents the true model parameters from TCTE, '$m_{O\text{-}H}$', '$m_{S\text{-}H}$', '$m_{O\text{-}R\text{-}H}$', '$m_{S\text{-}R\text{-}H}$' , stand for the initial iterates provided by the Hammersley point-set in its original, scrambled, randomness added to the original and randomness added to the scrambled forms. From the results it can be seen that the original version of the Hammersley point-set takes only 90 iterations to identify a starting solution in the C-C-D region, while the scrambled version takes 262. In order to compare their performance with the Mersenne-Twister uniform pseudo-random number generator, the QMC search stage was run with this generator 15,000 times. This has been done to get an average statistic for the number of iterations taken by the pseudo-random generator. The result of this numerical experiment can be seen in Fig. 4(a). From the figure it can be observed that pseudo-random generators can provide a 'lucky-hit', wherein, the starting solution can be obtained in just one iteration, or, they can be exorbitant, with the search stage consuming at least 106,074 iterations to identify a good initial iterate. On an average, the Mersenne-Twister generator took 9124 iterations to recognize a solution in the C-C-D hyper-volume. This result affirms the superior space-filling nature of the Hammersley point-set in comparison to a standard pseudo-random generator. Too many conclusions should not be drawn from the results obtained for '$m_{O\text{-}R\text{-}H}$' and '$m_{S\text{-}R\text{-}H}$', as, these MC-QMC point-sets were generated by adding pseudo-randomness to quasi-randomness. Hence, their performance should also be evaluated in terms of an average statistic for convergence.

'm_{GD}' represents the model parameters obtained at the end of the descent procedure. On an average, the descent scheme took 70 regularized Newton steps to converge to the final solution. Newton's method was implemented with quadratic line-search with q = 0.7. For the initial iterate provided by the QMC point-sets, Newton's method converged to the final solution in 7 steps without requiring regularization (q = 0) and line-search. Regularization and quadratic line-search were only needed for the starting solutions provided by the pseudo-random generator and the MC-QMC point-sets. However, to maintain the overall robustness of the proposed approach, regularization and quadratic line-search were incorporated into the descent procedure. The convergence criteria for the descent algorithm was set as $\left\| m_i - m_{i-1} \right\|_\infty \leq 0.0001$.

Model Parameters	x_S (m)	y_S (m)	z_S (m)	q_S / u_S (g / m)	θ_S (degrees)	# of iterations
m_t	**2000**	**5000**	**115**	**0.64**	**308.57**	**--------**
$m_{O\text{-}H}$	17.8	6015.62	178.6	0.904	294.5	90
$m_{S\text{-}H}$	52.2	6269.53	15.08	0.68	298.05	262
$m_{O\text{-}R\text{-}H}$	412.86	5508.3	66.42	0.51	292.98	1279
$m_{S\text{-}R\text{-}H}$	1020.28	5314.44	100.4	0.56	292.55	35,339
m_{GD}	***1905.36***	***4984.62***	***163.11***	***0.77***	***292.78***	***70***

Table. 2: Results at the end of the QMC search stage and the gradient descent procedure

A few other interesting results of inversion are shown in Figs. 4(b), 4(c), and 4(d). Fig. 4(b) depicts the solutions generated by the Mersenne-Twister generator during the search stage. From the figure it can be seen that the x and the y values of the initial iterates generated are distributed in an asymmetric manner around the true source location, while, the z values are distributed more uniformly about the true value. Along any z-plane, it can be observed that the starting solutions lie within a triangular region for the β_{QMC} value chosen. This behavior in 5D is in agreement with the earlier hypothesis in 2D that there exists a C-C-D region around the global minimum, and, as seen in Fig. 2(b), the region appears to have a triangular contour.

Fig. 4(c) shows the behavior of α and $\frac{\alpha \cdot s(\alpha)}{i(\alpha)}$ during the descent procedure when using 'm_{OH}' as the initial iterate. From the figure it can be seen that as $\alpha \to 0; \frac{\alpha \cdot s(\alpha)}{i(\alpha)} \to 0$. This demonstrates how the significance of the stabilizer fades as the gradient algorithm approaches the final solution. Fig. 4(d) shows the plume spread obtained using the predicted model parameters (m_{GD}). S_t (hexagon) and S_p (plus) denote the true and the predicted locations of the source. From the figure it can be concluded that the plume spread obtained from m_{GD} matches the sensor measurements far better than that observed in Fig. (1) (for true parameters – m_t).

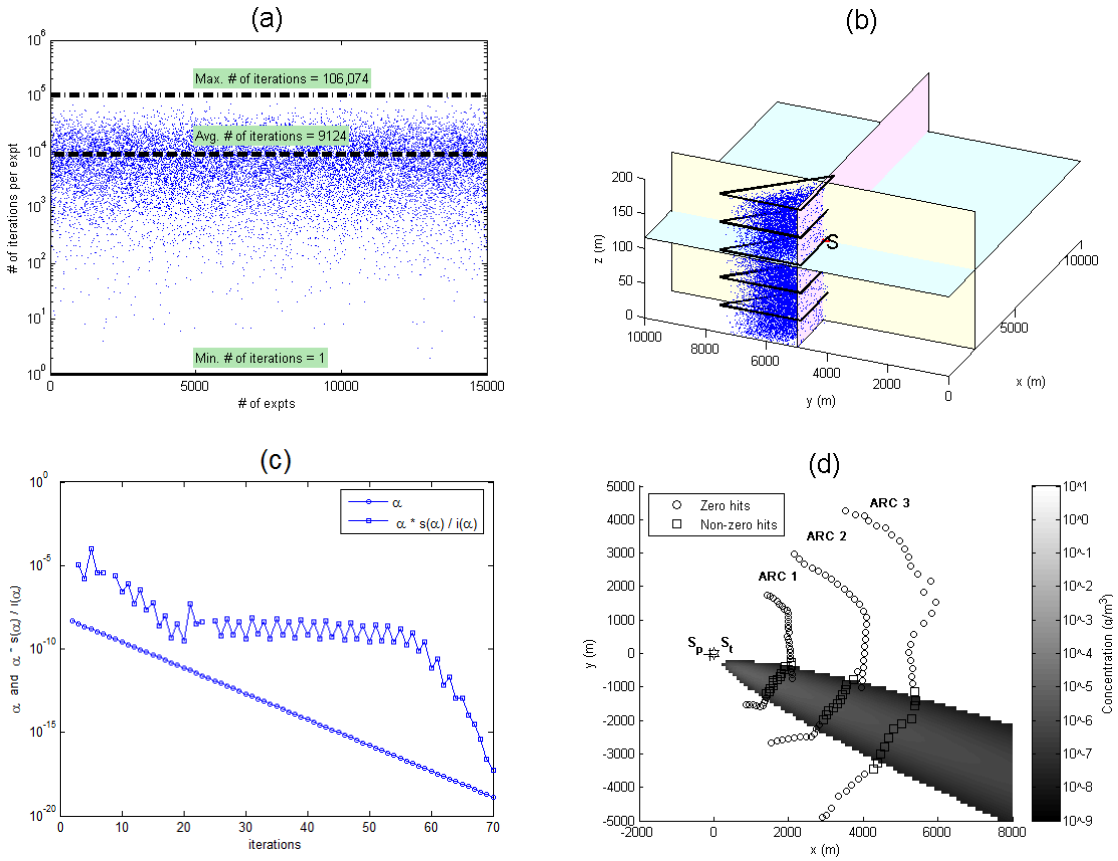

Fig. 4: (a) Iterations taken by the pseudo-random generator for 15,000 experiments, (b) Distribution of the x, y and z coordinates of the solution generated by the search stage using the Mersenne-Twister generator, (c) Behavior of the regularization parameter α and the ratio of the stabilizing and the misfit functionals in the descent algorithm with 'm_{OH}' as the starting iterate, (d) Plume spread predicted by the model parameters obtained from inversion (m_{GD})

6. Conclusions

The work presented describes an inversion technique to solve the atmospheric source characterization problem. A simple Gaussian plume model was adopted as the forward model. The approach proposed comprises of quasi-random sampling of the model parameter space and the subsequent application of gradient optimization. QMC sampling was performed using the Hammersley point-set in its original, scrambled and randomized form and regularized Newton's method with quadratic line-search was employed for gradient descent. A modified version of the Tikhonov stabilizing functional suited for

atmospheric inverse-source problems was used for regularization and the regularization parameter was updated adaptively in the descent algorithm. A few features of atmospheric source inversion problems that make the reconstruction procedure challenging are discussed and ways to tackle them are suggested. Prominent among them is the development of a new misfit functional based on the L_∞-norm of the ratio of the observed and predicted data that takes into account both the zero and non-zero hits recorded by the receptors. Additionally, the work presented highlights the advantages of using deterministic low-discrepancy sampling over the conventional pseudo-random sampling to solve atmospheric event reconstruction problems. Future work will investigate and document the correlation between the star-discrepancy of a point-set and its effectiveness in the sampling procedure.

References

[1] Akecelik, V., Biros, G., Draganescu, A., Ghattas, O., Hill, J., Waanders, B.V.B.: Inversion of airborne contaminants in a regional model. Lecture notes in computer science **3993** (2006) 481-488

[2] Allen, C.T., Haupt, S.E., Young, G.S.: Application of genetic algorithm-coupled receptor/dispersion model to the dipole pride 26 experiments. 14th Joint Conference on the Applications of Air Pollution Meteorology with the Air and Waste Management

[3] Allen, C.T., Young, G.S., Haupt, S.E.: Improving pollutant source characterization by better estimating wind direction with a genetic algorithm. Atmospheric Environment **41** (2007) 2283-2289

[4] Annunzio, A.J., Haupt, S.E., Young, G.S.: Source characterization and meteorology retrieval including atmospheric boundary layer depth using genetic algorithm. 10th Conference on Atmospheric Chemistry

[5] Aster, R.C., Borchers, B., Thurber, Clifford.: Parameter estimation and inverse problems

[6] Ballester, P.J., Carter, J.N.: Characterizing the parameter space of a highly nonlinear inverse problem. Inverse Problems in Science and Engineering **14** (2006) 171-191

[7] Beck, J.V., Woodbury, K.A.: Inverse problems and parameter estimation: integration of measurement and analysis. Meas. Sci. Technol. **9** (1998) 839-847

[8] Beychok, M.R.: Fundamentals of stack gas dispersion. ISBN 0-9644588-0-2

[9] Bocquet, M.: Reconstruction of an atmospheric tracer source using the principle of maximum entropy. I: Theory. Q. J. R. Meteorol Soc. **131** (2005) 2191-2208

[10] Bradley, M.N., Kosovic, B., Nasstrom, J.S.: Models and measurements: Complementary tools for predicting atmospheric dispersion and assessing the consequences of nuclear and radiological emergencies. International conference on monitoring, assessments, and uncertainties for nuclear and radiological emergency response (2005)

[11] Brown, M.J., Williams, M.D., Streit, G.E., Nelson, M., Linger, S.: An operational event reconstruction tool: Source inversion for biological agent detectors. 86th American Meteorological Society Annual Meeting (2006)

[12] Chow, F., Kosovic, B., Chan, S.T.: Source inversion for contaminant plume dispersion in urban environments using building-resolving simulations. 86th American Meteorological Society Annual Meeting (2006)

[13] Davoine, X., Bocquet, M.: Inverse modeling-based reconstruction of the Chernobyl source term available for long-range transport. Atmos. Chem. Phys. Discuss **7** (2007) 1-43

[14] Edwards, D.: Practical sampling for ray-based rendering. A thesis submitted to the faculty of The University of Utah in partial fulfillment of the requirements for the degree of Doctor of Philosophy, School of Computing

[15] Frandsen, P.E., Jonasson, K., Nielsen, H.B., Tingleff, O.: Unconstrained Optimization. Informatics and Mathematical Modeling, Technical University of Denmark

[16] Gryning, S.E., Lyck, E.: The Copenhagen tracer experiments: Reporting measurements. Riso National Laboratory, Roskilde, 1998

[17] Hanson, K.M.: Quasi-Monte Carlo: Halftoning in high dimensions? Proc. SPIE **5016** (2003) 161-172

[18] Haupt, S.E., Haupt, R.L., Young, G.S.: Using genetic algorithms in chem-bio defense applications. Proceedings of the 2007 ECSIS Symposium on Bio-inspired, Learning, and Intelligent Systems for Security (2007) 151-154

[19] Haupt, S.E., Young, G.S.: Paradigms for source characterization. 88th American Meteorological Society Annual Meeting (2008)
[20] Hogan, W.R., Cooper, G.F., Wagner, M.M., Wallstrom, G.L.: An inversion Gaussian plume model for estimating the location and amount of release of airborne agents from downwind atmospheric concentrations. The RODS laboratory, University of Pittsburgh
[21] Houweling, S., Kamsinki, T., Dentener, F., Lelieveld, J., Heimann, M.: Inverse modeling of methane sources and sinks using the adjoint of a global transport model. Journal of Geophysical Research **104** (1999) 26,137-26,160
[22] Islam, M.A.: Application of the Gaussian plume model to determine the location of an unknown emission source. Water, Air and Soil Pollution **112** (1999) 241-245
[23] Kelley, C.T.: Solving nonlinear equations with Newton's method. Fundamentals of Algorithms, SIAM
[24] Kennett, B.L.N.: Consistency regions in non-linear inversion. Geophys. J. Int. **157** (2004) 583-588
[25] Khemka, A., Bouman, C.A., Bell, M.R: Inverse problems in atmospheric dispersion with randomly scattered sensors. Digital Signal Processing **16** (2006) 638-651
[26] Lemieux, C.: Monte Carlo and Quasi-Monte Carlo Sampling. Springer
[27] Lomax, A., Sneider, R.: Identifying sets of acceptable solutions to non-linear, geophysical inverse problems which have complicated misfit functions. Nonlinear Processes in Geophysics **2** (1995) 222-227
[28] Long, K.J., Haupt, S.E., Young, G.S., Allen, C.T.: Characterizing contaminant source and meteorological forcing using data assimilation with a genetic algorithm. 86th American Meteorological Society Annual Meeting (2006)
[29] Mosegaard, K., Trantola, A.: Monte Carlo sampling of solutions to inverse problems. Journal of Geophysics Research **100** (1995) 12,431-12,447
[30] Niederreiter, H.: Random number generation and Quasi-Monte Carlo methods. CBMS-NSF Regional Conference Series in Applied Mathematic
[31] Scales, J.A., Tenorio, L.: Prior information and uncertainty in inverse problems. Geophysics **66** (2001) 389-397
[32] Sambridge, M., Beghein, C., Simons, F.J., Sneider, R.: How do we understand and visualize uncertainty? The Leading Edge (2006) 542-546
[33] Sambridge, M.: Inverse problems in a nutshell. Center for Advanced Data Inference, Research School of Earth Sciences, Australian National University, ACT 0200, Australia
[34] Senocak, I., Hengartner, N.W., Short, M.B., Daniel, B.W.: Stochastic event reconstruction of atmospheric contaminant dispersion using Bayesian inference. Atmospheric Environment **42** (2008) 7718-7727
[35] Sneider, R.: The role of nonlineaity in inverse problems. Inverse Problems **14** (1998) 387-404
[36] Sambridge, M., Mosegaard, K..: Monte Carlo methods in geophysical inverse problems. Reviews of Geophysics **40** (2002) 1-29
[37] Sambridge, M.: Finding acceptable solutions in nonlinear inverse problems using a neighborhood algorithm. Inverse Problems **17** (2001) 387-403
[38] Storch, R.B., Pimentel., L.C.G., Orlande, H.R.B.: Identification of atmospheric boundary layer parameters by inverse problem. Atmospheric Environment **41** (2007) 1417-1425
[39] Thomson, L.C., Hirst, B., Gibson, G., Gillespie, S., Jonathan, P., Skeldon, K.D., Padgett, M.J.: An improved algorithm for locating a gas source using inverse methods. Atmospheric Environment **41** (2007) 1128-1134
[40] Trantola, A.: Inverse problem theory and methods for model parameter estimation. SIAM
[41] Turner, B.D.: Workbook of atmospheric dispersion estimates – An introduction to dispersion modeling. Lewis Publishers
[42] Vogel, C.R.: Computational methods for inverse problems. Frontiers in applied mathematics, SIAM
[43] Wirgin, A.: The inverse crime. *LMA/CNRS, 31 chemin Joseph Aiguier, 13402 Marseille cedex 20, France
[44] Zajic, D., Brown, M.J.: Source inversion in cities using the collector footprint methodology. 88th American Meteorological Society Annual Meeting (2008)
[45] Zbinsky, Z.B.: Stochastic adaptive search for global optimization. Kluwer Academinc Publishers
[46] Zhadanov, M.S.: Geophysical inverse theory and regularization problems. Methods in Geochemistry and Geophysics, **36**, ELSEVIER

Authors	Model Parameters (m)	Forward Model (A)	Inversion Technique	Validation Procedure	Application	Max. Grid Size	# of runs	Performance
Akcelik et al, [1]	Strength (Q_s)	Steady laminar incompressible Navier-Stokes solver + ADE	Adjoint Method	Synthetic data without noise	Contamination event in the Greater Los Angeles Basin (GLAB)	361× 121× 21		1) 917,301 concentration unknowns per time step 2) Total of 40 time steps 74×10^6 space-time variables
Annunzio et al, [4]	Location (x_s, y_s,z_s), Strength (Q_s), Wind speed (u_s) Wind direction (θ_s) Boundary layer depth (δ_s)	Gaussian puff	Genetic Algorithm	Synthetic data without noise	Source characterization of atmospheric contaminant dispersion including the boundary layer depth			
Brown et al, [11]	Location (x_s, y_s), Strength (Q_s)	Gaussian plume model	Detector Footprint Methodology	Synthetic data with and without noise	Event reconstruction of atmospheric contaminant dispersion			
Chow et al, [12]	Location (x_s, y_s, ,z_s), Strength (Q_s)	FEM3MP – 3D incompressible Navier-Stokes finite element code	Bayesian Inference + MCMC	1) Synthetic data with and without noise around a cube 2) Joint Urban 2003 IOP3	Event reconstruction in urban environments using building resolving simulations	132× 146× 30 for JU2003 – IOP3		1) 2560 forward runs 2) Total computation time of over 12 hours using 1024 2.4GHz Xeon processors – equivalent to 17 days on 32 processors
Davoine and Bocquet, [13]	z_s – Effective source altitude t_s – Temporal release profile	Chemistry Transport Model (CTM) – POLAIR 3D	Adjoint Method		Reconstruction of Chernobyl accident source term			
Haupt et al, [18]	Location (x_s, y_s), Strength (Q_s), Wind speed (u_s) Wind direction (θ_s) Stability Class	Gaussian Plume model	Genetic Algorithm	Synthetic data without noise	Event reconstruction of atmospheric contaminant dispersion	32× 32	10	1) 2000 generations for the meteorological parameters 2) 10,000 generations for x_s, y_s, Q_s, θ_s & stability

Table. 1: Salient features of the various inversion techniques used to solve atmospheric source characterization problems

Authors	Model Parameters (m)	Forward Model (A)	Inversion Technique	Validation Procedure	Application	Max. Grid Size	# of runs	Performance
Houweling et al, [21]	$f_{j,m}$ – Integrated surface emission over region 'j' & month 'm' s_{OH} – Parameterization for chemical removal of methane with hydroxyl radical s_{stea} – Stratospheric methane loss c_0 – Global mean methane concentration	Global Atmospheric Chemistry Transport Model (CTM)	Adjoint Method	National Oceanic and Atmospheric Administration (NOAA) / Climate Monitoring and Diagnostics Laboratory (CMDL) cooperative air sampling network	Study of global-scale sources and sinks of methane			
Khemka et al, [25]	Location (x_s, y_s, ,z_s), Strength (Q_s)	Gaussian dispersion model	Expectation – Maximization algorithm (EM)	Synthetic data without noise	Source characterization using randomly scattered sensors			
Long et al, [28]	Location (x_s, y_s), Strength (Q_s), Wind direction (θ_s)	Gaussian puff	Genetic Algorithm + Simplex Optimization (Nelder-Mead)	Synthetic data without noise – Identical Twin Experiment		32× 32	10	1) # of chromosomes = 1200 2) Mutation Rate = 0.015 3) 100 GA iterations
Senocak et al, [34]	Location (x_s, y_s, ,z_s), Strength (Q_s), Wind speed (u_s) Wind direction (θ_s)	Gaussian plume model	Bayesian Inference + MCMC	Copenhagen Tracer Experiments, (Erik & Lyck, 2002)	Stochastic event reconstruction of atmospheric contaminant dispersion			50,000 MCMC evaluations
Storch et al, [38]	Longitudinal diffusivity (K_{xx}), Friction velocity (u^*), Monin-Obukhov length (L), Surface roughness (z_0)	2D advection – diffusion equation (ADE)	Least squares minimization by Levenberg-Marquardt method	Copenhagen Tracer experiments	Identification of atmospheric boundary layer parameters			
Thomson et al, [39]	Location (x_s, y_s, ,z_s), Strength (Q_s)	Gaussian plume model	Simulated Annealing (SA)	Simulated experimental data	Use of atmospheric ethane concentration to locate ground-level sources	16× 16		4×10^6 iterations

Table. 1: Salient features of the various inversion techniques used to solve atmospheric source characterization problems